Evolutionary Ecology Research, 2010, **12**: 413–434

Adaptive dynamics of temperate phages

Thomas Evans[1], Roger G. Bowers[1] and Martin Mortimer[2]

[1]*Department of Mathematical Sciences, Division of Applied Mathematics and*
[2]*School of Biological Sciences, The University of Liverpool, Liverpool, UK*

ABSTRACT

Background: Phages are viruses that infect bacteria. Following infection of a bacterial cell, temperate phages may replicate via one of two distinct pathways, known as lysis and lysogeny. Lysis involves the synthesis of a large number of phage particles, which are then released when the host cell is lysed (i.e. burst open). In lysogenic reproduction, the infecting phage genome is inserted into the genome of the host cell (forming a lysogen cell), and is then replicated via normal bacterial cell division. Lysogens may also undergo lysis in a process known as induction.

Questions: How does the virulence of temperate phages evolve over time? How do environmental conditions influence this evolution?

Mathematical methods: The methods of adaptive dynamics are used to determine the location and nature of evolutionary singularities. These singularities determine the direction in which evolution proceeds.

Key assumptions: Over long periods of time, the probability of lysogeny (p) and the induction rate (i) within a population of temperate phages may evolve via small mutations. There is a trade-off relationship between the parameters p and i.

Predictions: The evolutionary singularities may be either attractors or repellors, depending on whether the trade-off cost is accelerating or decelerating. Marginally ESS attractors, which are convergent stable and borderline evolutionarily stable, may also occur. Branching point singularities, which are associated with speciation, do not occur in this framework. A decrease in the level of resources in the environment per susceptible bacterium cell results in a shift towards greater phage virulence.

Keywords: evolution of virulence, lysis, lysogeny, singularities, trade-offs.

1. INTRODUCTION

Temperate bacteriophages (phages) select between two developmental pathways following adsorption to a host bacterial cell. These pathways are known as lysis and lysogeny. During lysis, many copies of the phage are produced and then released when the cell is lysed. If the lysogenic pathway is selected, the phage genome is inserted into the bacterial genome and

Correspondence: T. Evans, Department of Mathematical Sciences, Division of Applied Mathematics, Mathematical Sciences Building, The University of Liverpool, Liverpool L69 3BX, UK. e-mail: t.w.evans@liv.ac.uk

replicated passively every time the cell divides. Following creation of a lysogen, a process known as induction may be initiated at a later time, leading to lysis of the host cell and the release of new phage particles. In the extensively studied temperate phage lambda, an increasingly well understood molecular switching mechanism selects between the two pathways, and can also initiate induction of a lysogen (Ptashne, 2004; Evans *et al.*, 2007). For the purposes of this paper, the behaviour of the switch is characterized by two parameters: the probability of lysogeny (p) and the lysogen induction rate (i).

Using a chemostat model, Mittler (1996) investigated the outcome of pairwise competition between phage strains with different (fixed) values of i and p. In this model, strains with low values of both p and i were found to be strong competitors and generally able to invade when rare. It was speculated that this may be the reason why well-studied temperate phages such as phage lambda, Mu, and P1 have all evolved to have probabilities of lysogeny lower than 0.5 and induction rates of the order of 0.00001 per hour (Rosner, 1972; Kourilsky, 1973; Howe and Bade, 1975); in theory, p could be anywhere between 0 and 1, and i could be any non-negative number. Our aim in this paper is to investigate the evolution of the parameters p and i.

The theory of adaptive dynamics (Geritz *et al.*, 1998) provides a framework for modelling the evolution of a single trait within a population. Initially, there is a resident population of identical individuals at equilibrium, but small mutations can occur in this population. If a few mutants emerge, they may simply die out so that the previous equilibrium is restored; alternatively, their population may grow so that they eventually replace the existing resident population. Evolution thus proceeds via a series of small mutations. Evolutionary singularities play a central role, and they can be of various types corresponding to very different evolutionary outcomes. They can be attractors (commonly associated with the long-term emergence of intermediate trait values), repellors (evolution towards other singularities or 'extreme' trait values) or branching points (dimorphisms/trait co-existence).

In the present paper, we apply the methods of adaptive dynamics to the Mittler (1996) model. Our aim is to determine which evolutionary outcomes are possible in this model, and to interpret these outcomes biologically. In common with applications in many other areas (e.g. Bowers and White, 2002; de Mazancourt and Dieckmann, 2004), we introduce the constraint that $i = f(p)$ for some function f. We present some analytical results that can be used to locate and classify the evolutionary singularities of the system, and we explore the importance of the shape of the function f in determining the number and nature of the singularities. We also investigate how the locations of evolutionary singularities change when the supply of sensitive bacteria and resources changes. The theoretical results obtained will be illustrated with a number of examples.

2. A TWO-STRAIN MODEL

The chemostat model (Mittler, 1996) consists of two phage strains (P_1 and P_2) and their associated host lysogens (L_1 and L_2 respectively). There is also a flow of sensitive bacteria (S) and resources (R) into the chemostat. Following adsorption of a P_1 phage to a sensitive bacterial cell, an L_1 lysogen may be formed, while adsorption of a P_2 phage may result in the formation of an L_2 lysogen. Strains 1 and 2 differ only in their probabilities of lysogeny (p_1 and p_2 respectively) and their induction rates (i_1 and i_2). The model is given below:

$$\frac{dR}{dt} = \omega(R_0 - R) - \varepsilon r (S + L_1 + L_2) R/(R + k) \tag{1}$$

$$\frac{dS}{dt} = \omega(S_0 - S) + rSR/(R+k) + \xi(L_1 + L_2) - \delta SP_1 - \delta SP_2 \quad (2)$$

$$\frac{dL_1}{dt} = p_1\delta SP_1 + rL_1R/(R+k) - i_1L_1 - \xi L_1 - \omega L_1 \quad (3)$$

$$\frac{dL_2}{dt} = p_2\delta SP_2 + rL_2R/(R+k) - i_2L_2 - \xi L_2 - \omega L_2 \quad (4)$$

$$\frac{dP_1}{dt} = (1-p_1)\beta\delta SP_1 + \beta i_1L_1 - \delta(S + L_1 + L_2)P_1 - \omega P_1 \quad (5)$$

$$\frac{dP_2}{dt} = (1-p_2)\beta\delta SP_2 + \beta i_2L_2 - \delta(S + L_1 + L_2)P_2 - \omega P_2 \quad (6)$$

Here, ω is the chemostat flow rate, and R_0 and S_0 are the concentrations of resource and susceptible bacteria respectively in the input reservoir. Thus resources and susceptible bacteria enter the habitat at rates of ωR_0 and ωS_0 respectively. Similarly, all of the constituent species within the habitat are washed out at a rate proportional to ω. The growth rates of susceptible bacteria and lysogens are related to the availability of resources via the Monod function $rR/(R+k)$ (Monod, 1949), where r is the maximal growth rate and k is the resource concentration at which cells grow at half their maximal growth rate. The parameter ε measures how many resource particles are necessary to make a new bacterium. The parameter δ is associated with the rate at which free phages encounter and adsorb to bacterial cells. The probability that a phage of strain P_1 (P_2) will form a lysogen with its bacterial host is denoted p_1 (p_2), and i_1 (i_2) is the spontaneous induction rate for a lysogen of type L_1 (L_2). Those phages that do not form lysogens will enter the lytic cycle immediately after adsorption to a susceptible bacterial cell. Following lysis of an infected cell, the number of newly created phages is given by the burst size, β. The parameter ξ allows for the event of a lysogen losing its prophage and thus returning to its original state of a susceptible bacteria. The model assumes that lysogens are immune to further infection by either phage strain.

Note that equations (5) and (6) include the additional terms $-\delta SP_1$ and $-\delta SP_2$ respectively, compared with the original model given in Mittler (1996). These terms represent the loss of free phage particles that adsorb to and infect susceptible cells.

Now suppose that there is a resident population of strain x and its lysogen (with parameters p_1 and i_1) at equilibrium, and that strain y (with parameters p_2 and i_2) is a rare mutant. Define the function $s_x(y)$ as follows:

$$s_x(y) = Q(p_1, i_1)^2\gamma(p_1, i_1) + Q(p_1, i_1)i_2 - Q(p_1, i_1)\,\mu(p_1, i_1)p_2 \quad (7)$$

where

$$\gamma(p, i) = P^*/\beta L^*$$
$$\mu(p, i) = \delta S^* P^*/L^*$$
$$Q(p, i) = (\beta p\delta S^* P^* - \beta i L^*)/P^*$$

and S^*, L^*, and P^* are the equilibrium densities of S, L, and P for a resident phage with parameters p and i. Then, strain y and its lysogen will be able to invade when rare if $s_x(y) > 0$ (Mittler, 1996) (see Appendix A).

By setting the right-hand side of equation (5) equal to zero, and re-arranging, the expression for $Q(p, i)$ can be shown to be equivalent to:

$$Q(p, i) = \beta\delta S^* - \delta(S^* + L^*) - \omega$$

and so $Q(p, i)$ can be interpreted as the net rate at which the phage population would increase if the the probability of lysogeny were zero.

2.1. The significance of the function Q

We now summarize some observations regarding the function Q, which were stated without proof in Mittler (1996). First, if $Q(p_1, i_1)$ and $Q(p_2, i_2)$ have opposite signs, then both strains can invade when rare and the two strains will co-exist. On the other hand, if $Q(p_1, i_1)$ and $Q(p_2, i_2)$ have the same sign, then the strain with the lower value of $|Q|$ can invade when rare, while the strain with the greater value of $|Q|$ cannot invade when rare. Furthermore, if the resident has $Q = 0$, then invasion is not possible by any mutant strain; if the mutant has $Q = 0$, then it can invade any resident with $Q \neq 0$, but will not drive it to extinction. These statements can be verified for our modified model as follows.

By setting equations (1), (2), (3), and (5) all equal to zero (with $P_2 = L_2 = 0$) and applying the implicit function theorem, it can be seen that the resident equilibrium populations (R^*, S^*, L_1^*, P_1^*) are all continuous and continuously differentiable functions of i and p: the Jacobian is non-singular since we take the equilibrium to be stable. It follows that $Q(i, p)$ is also continuous and continuously differentiable. Furthermore, it can also be seen from the same set of equations that for any constant k, the line $Q(i, p) = k$ is unique (see Appendix B). Any cross-section of the surface $Q(i, p)$ except those corresponding to these lines takes any value of Q only once. Thus the contour plot in Fig. 1 of the Q function for the parameter values given in Mittler (1996) shows steady decrease through $Q = 0$.

Since $s_x(x) = 0$, we can re-write (7) as:

$$\begin{aligned} s_x(y) &= s_x(y) - s_x(x) \\ &= Q_1[i_2 - i_1 - \mu_1(p_2 - p_1)] \end{aligned} \tag{8}$$

Suppose that the resident lies on the line $Q = 0$ (i.e. $Q_1 = 0$). Then using the above expression we see that $s_x(y) = 0$ irrespective of the mutant parameters p_2 and i_2, and therefore no mutant can invade.

Now suppose that $Q_A > 0$, $Q_B > 0$, and $Q_A > Q_B$. There are three cases to consider: (i) $p_B > p_A$; (ii) $p_B < p_A$; (iii) $p_B = p_A$. These are dealt with in turn below.

Suppose first that $p_B > p_A$, in which case we must have $i_B > i_A$ as well (since $Q_B < Q_A$). If A is the resident and B is the mutant, then we have $s_A(B) = Q_A(i_B - i_A - \mu_A\ (p_B - p_A))$, where Q_A, μ_A, $(i_B - i_A)$, and $(p_B - p_A)$ are all positive. Now the slope of the line $Q = Q_A$ (which is equal to μ_A) must be less than the slope of the line through A and B. Thus

$$\mu_A < \frac{i_B - i_A}{p_B - p_A} \tag{9}$$

and hence $s_A(B) > 0$. On the other hand, if B is the resident and A is the mutant, we have $s_B(A) = Q_B(i_A - i_B - \mu_B(p_A - p_B))$, where Q_B and μ_B are positive, while $(i_A - i_B)$ and $(p_A - p_B)$ are negative. Since the Q lines cannot intersect for feasible i and p, the gradient of

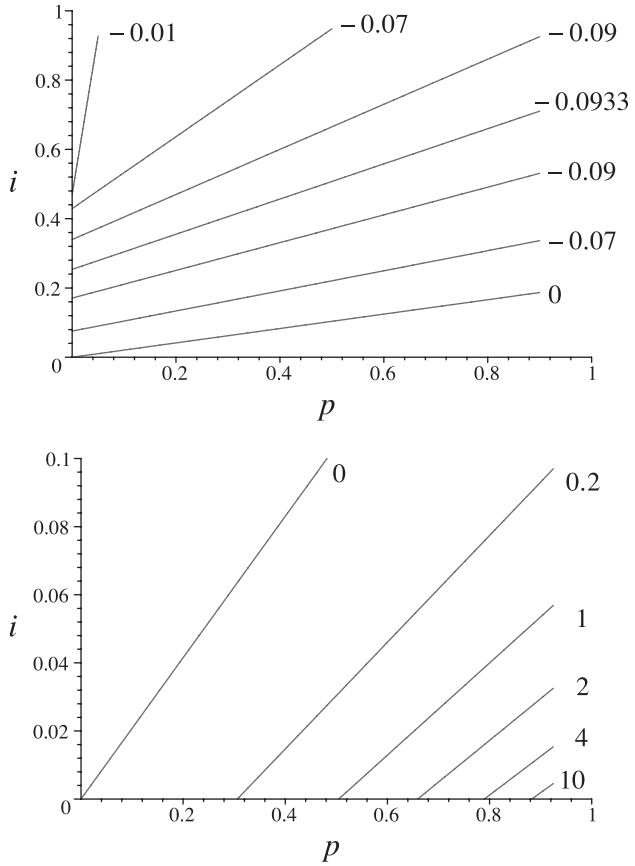

Fig. 1. Contour plots for the function Q. Each contour is labelled with its respective Q value. The contours are all straight lines, and the gradient of each line is equal to the value of the function μ along that line. Parameter values: $R_0 = 100\ \mu g \cdot ml^{-1}$, $S_0 = 2 \times 108\ \mu g \cdot ml^{-1}$, $\delta = 10^{-9}\ ml \cdot h^{-1}$, $\beta = 100$, $\xi = 0.0001 \cdot h^{-1}$, $r = 0.7 \cdot h^{-1}$, $k = 4.0\ \mu g \cdot ml^{-1}$, $\varepsilon = 5 \times 10^{-7}\ \mu g$, $\omega = 0.2 \cdot h^{-1}$.

the line $Q = Q_B$ (i.e. μ_B) must be less than the gradient of the line through A and B (i.e. $(i_A - i_B)/(p_A - p_B)$), and so $s_B(A) < 0$.

Now let $p_B < p_A$ and $i_B > i_A$. We have $s_A(B) = Q_A\,(i_B - i_A - \mu_A\,(p_B - p_A))$, where Q_A, μ_A, and $(i_B - i_A)$ are positive, and $(p_B - p_A)$ is negative; hence $s_A(B)$ is positive. We also have $s_B(A) = Q_B(i_A - i_B - \mu_B(p_A - p_B))$, which is clearly negative.

Now let $p_B > p_A$ and $i_B < i_A$. Then,

$$\mu_A > \frac{i_A - i_B}{p_A - p_B} \qquad \text{and} \qquad \mu_B > \frac{i_A - i_B}{p_A - p_B} \tag{10}$$

and it follows (using (8)) that $s_A(B) > 0$ and $s_B(A) < 0$.

Now let $p_B = p_A$, in which case we must have $i_B > i_A$ (since $Q_B < Q_A$). Using (8), it is immediately clear that $s_A(B) > 0$ and $s_B(A) < 0$.

The arguments above show that for any two strains A and B with $0 < Q_B < Q_A$, it must be the case that $s_A(B) > 0$ and $s_B(A) < 0$. Similar reasoning can be used to show that for any two strains A and B with $Q_B < Q_A < 0$, we must have $s_B(A) > 0$ and $s_A(B) < 0$.

Finally, suppose that $Q_A < 0$ and $Q_B > 0$, and let $p_A < p_B$ and $i_A < i_B$. Then by considering the slopes of the lines $Q = Q_A$, $Q = Q_B$, and the line through A and B, we have:

$$\mu_A > \frac{i_B - i_A}{p_B - p_A} \tag{11}$$

and

$$\mu_B > \frac{i_B - i_A}{p_B - p_A} \tag{12}$$

It follows that both $s_A(B)$ and $s_B(A)$ are positive. Similar reasoning can be used to show that if $Q_A < 0$ and $Q_B > 0$, then both $s_A(B)$ and $s_B(A)$ are positive for the cases: (i) $p_A < p_B$ and $i_A > i_B$; (ii) $p_A > p_B$ and $i_A > i_B$; and (iii) $p_A > p_B$ and $i_A < i_B$. This completes the proof of Mittler's assertions.

2.2. Introducing a trade-off between *i* and *p*

The approach used by Mittler (1996) involves modelling the outcome of competition between two fixed phage strains, whereas the adaptive dynamics approach enables repeated mutation and selection to be modelled. We aim to investigate long-term evolutionary outcomes for temperate phages using this approach, in the context of an equitable environment.

We assume that there is a function f such that $i = f(p)$. This represents constraints in the system or trade-offs corresponding to cost–benefit dependencies (for general discussions, see de Mazancourt and Dieckmann, 2004; Rueffler *et al.*, 2004; Bowers *et al.*, 2005). The assumption of a biological relationship between the induction rate and the probability of lysogeny is reasonable since both are partly determined by the regulation of the genetic 'switch' on the lambda genome (Ptashne, 2004); however, the nature of this relationship has not been investigated experimentally. In this paper, several different f functions will be considered. It would also be instructive to investigate the situation where i and p are not constrained in this way, and can therefore evolve independently, but this is beyond the scope of the present paper.

Substituting $i = f(p)$ in (7), we obtain the following function:

$$s_{p1}(p_2) = Q(p_1)^2 \gamma(p_1) + Q(p_1) f(p_2) - Q(p_1)\mu(p_1)p_2 \tag{13}$$

We shall refer to $s_{p1}(p_2)$ as the mutant's fitness function, since it is (by the argument of Appendix A) sign-equivalent to the dominant eigenvalue of the invasion Jacobian. This eigenvalue is taken as the standard definition of fitness (Geritz *et al.*, 1998), but any sign-equivalent quantity is acceptable.

Since $s_{p1}(p_1) = 0$, we can re-write (13) as:

$$\begin{aligned} s_{p1}(p_2) &= s_{p1}(p_2) - s_{p1}(p_1) \\ &= Q(p_1)\,[f(p_2) - f(p_1) - \mu(p_1)\,(p_2 - p_1)] \end{aligned} \tag{14}$$

From (14) we see that a cost–benefit interpretation of $i = f(p)$ suggests $f'(p) > 0$; otherwise, both contributions in the second factor will have the same sign. The sign of $Q(p_1)$ plays a role here as discussed later.

2.3. Location of singularities

An evolutionary singularity p^* occurs at any point at which the partial derivative $\partial s_{p1}(p_2)/\partial p_2$ evaluated at $p_1 = p_2 = p^*$ is equal to zero. At such a point, the partial derivative $\partial s_{p1}(p_2)/\partial p_1$ will also be zero (Geritz *et al.*, 1998). Differentiating (14) with respect to p_2 and setting this equal to zero, we have

$$Q(p^*)[f'(p^*) - \mu(p^*)] = 0 \tag{15}$$

and so there is a singularity at any point p^* where one of the following expressions holds:

$$Q(p^*) = 0 \tag{16}$$

or

$$f'(p^*) = \mu(p^*) \tag{17}$$

The expression $Q(p, i) = 0$ describes a straight line in (p, i) space (see Appendix B). Condition (16) indicates that there will be a singularity at any point of intersection between the trade-off function and the line $Q(p, i) = 0$. Condition (17) tells us that there will be a singularity at any point at which the gradient of the trade-off function is equal to the value of μ. These are new results that can be used to locate all the evolutionary singularities easily.

2.4. Classification of singularities

The location of the singularities can be represented graphically using a pairwise invasibility plot (PIP) (Geritz *et al.*, 1998). These show the sign of the mutant's fitness for all possible combinations of p_1 and p_2. The mutant's fitness along the leading diagonal is always zero, because the resident population is at equilibrium and mutant and invader are identical. Evolutionary singularities occur at any point of intersection between the leading diagonal and another line along which the mutant's fitness is zero, while the pattern of signs around a singularity determines the nature of the singularity (Geritz *et al.*, 1998).

According to where (and whether) the trade-off function intersects the $Q = 0$ line on the i–p plane, the PIP is partitioned into blocks where the mutant and the resident have Q values of the same sign or of opposite signs; see Fig. 2 for an example of this. In blocks where the Q values have opposite signs, the mutant can invade; these regions are labelled '+' in the PIP. In blocks where the Q values have the same sign, the mutant can invade if and only if its absolute value is less than that of the resident. This is an optimization principle (the absolute value of Q is minimized) and induces a skew symmetric block in the PIP such that '+' mirrors into '−' and vice versa (Metz *et al.*, 2008).

As an example of the way in which the signs in the PIP can be determined, consider a resident phage with probability of lysogeny in the region of $p = 0.4$ in Fig. 2b. A mutant with a slightly higher value of p will lie closer to the $Q = 0$ line and have a smaller value of $|Q|$; therefore, it will be able to invade when rare. On the other hand, a mutant with a slightly lower value of p will have a greater value of $|Q|$ and so will not be able to invade. Thus, in the lower left block in the PIP (Fig. 2a) there is a '+' above and a '−' below the main diagonal.

There are two types of singularity to consider: (i) $Q = 0$ (for which (16) is satisfied) and (ii) $Q \neq 0$ (which satisfies (17)). It is seen directly from the invasion fitness in (13) that a resident with $Q = 0$ is singular and is a marginal ESS globally, since all mutants have zero

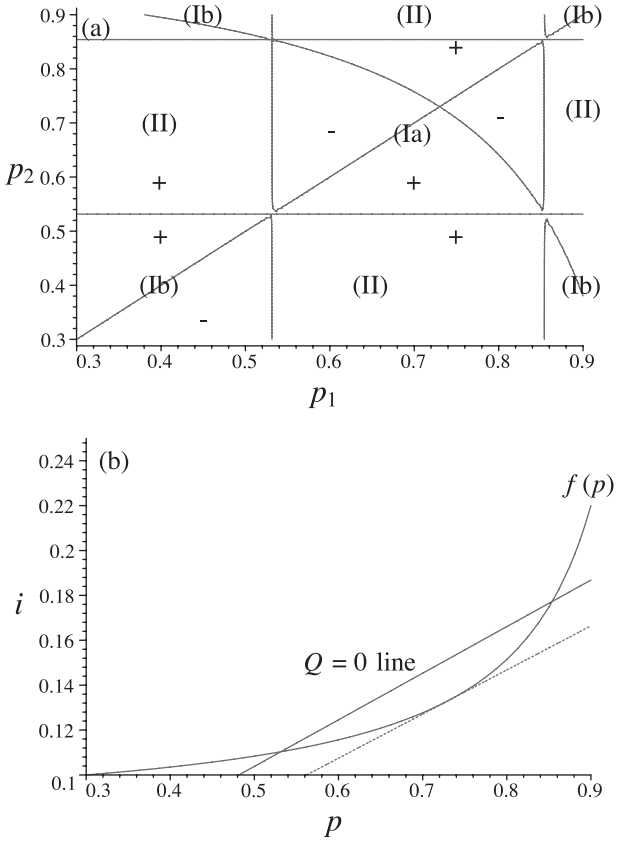

Fig. 2. The PIP in (a) is partitioned into blocks that are determined by the locations and intersection points of the line $Q = 0$ and the trade-off f in (b). In the blocks labelled (I), Q_1 and Q_2 have the same sign [I(a): both positive; I(b): both negative], $|Q|$ is minimized and hence the PIP is skew symmetric. In the blocks labelled (II), Q_1 and Q_2 have opposite signs and so the rare strain invades and the sign in the PIP is '+'. The tangent to the trade-off at the singularity is shown in (b) and coincides with a contour of the function Q.

invasion fitness. This amounts to a vertical invasion boundary on the PIP (which delineates the blocks described above). There are two possible sign configurations around a vertical line at the singularity – one with mutual invasibility and one without. However, when the trade-off intersects the $Q = 0$ line, there are strategies in the neighbourhood of the singularity that have Q values with opposite signs and therefore invade one another. This shows that the mutually invasible sign configuration is the only possibility in this model, and the singularity must also be convergence stable.

Within the skew symmetric blocks, evolution minimizes the value of $|Q|$. Therefore, a strategy that minimizes $|Q|$ is singular and is a locally optimal strategy, which is necessarily a convergence stable ESS. A strategy that maximizes $|Q|$ is also singular and is a locally pessimal strategy, which is necessarily not convergence stable and not an ESS. These types of singularity satisfy equation (17) (an example is shown in Fig. 2b, in which the tangent to the trade-off curve at the singularity coincides with a contour of the function Q). In both cases, there is no mutual invasibility and no mutual exclusion. It follows that above the $Q = 0$ line

convex trade-offs can minimize $|Q|$, while below the $Q = 0$ line concave trade-offs can minimize $|Q|$. Hence we can make the following statements:

$$Q(p^*) < 0,\ f''(p^*) > 0 \Rightarrow p^* \text{ is an attractor (ESS, CS)} \tag{18}$$

$$Q(p^*) < 0,\ f''(p^*) < 0 \Rightarrow p^* \text{ is a repellor (not ESS, not CS)} \tag{19}$$

$$Q(p^*) > 0,\ f''(p^*) > 0 \Rightarrow p^* \text{ is a repellor (not ESS, not CS)} \tag{20}$$

$$Q(p^*) > 0,\ f''(p^*) < 0 \Rightarrow p^* \text{ is an attractor (ESS, CS)} \tag{21}$$

Note (see (14) and the subsequent discussion) that if $Q > 0$, then an increase in i is a benefit and an increase in p is a cost; on the other hand, if $Q < 0$, then an increase in i is a benefit while an increase in p is a cost. Therefore, the above conditions can be re-written as:

f deceleratingly costly $\Rightarrow p^*$ is a repellor (not ESS, not CS)

f acceleratingly costly $\Rightarrow p^*$ is an attractor (ESS, CS)

3. SOME EXAMPLES

Here we present four examples that illustrate how the use of different trade-off curves can result in different numbers and types of singularities. Figure 1 shows some contours of the function Q for our chosen set of parameter values, and in particular shows the location of the line $Q = 0$. The general form of the trade-off functions used is as follows (White *et al.*, 2006):

$$f(p) = i_{\max} - \frac{(i_{\max} - i_{\min})\left(1 - \dfrac{p - p_{\min}}{p_{\max} - p_{\min}}\right)}{\left(1 + \dfrac{\alpha(p - p_{\min})}{p_{\max} - p_{\min}}\right)} \tag{22}$$

The value of the parameter α determines the curvature of the trade-off function. The value of α is taken to lie in the interval $(-1, \infty)$. If α lies in $(0, \infty)$, the trade-off is acceleratingly costly. If α lies in $(-1, 0)$, the trade-off is deceleratingly costly.

For each example below we use a PIP and a plot of the line $Q = 0$ and the trade-off function to illustrate the way that the singularities shown in the PIP correspond to different points along the trade-off function. We also show the results of simulating the mutation–selection process in a multi-strain model, to show how the resident strategy evolves either towards an attractor or away from a repellor (Bowers *et al.*, 2005; Miller *et al.*, 2005; White and Bowers, 2005).

3.1. An attractor

In this example, the PIP (Fig. 3a) shows that there is a singularity near $p = 0.6$. The pattern of signs around the singularity (minus signs above and below, plus signs to the left and right) indicates that it is an attractor.

Figure 3b shows the trade off function and the $Q = 0$ line in (p, i) space. The point p^* on the trade-off curve at which the value of $|Q|$ is minimized corresponds to the attractor identified in the PIP, in accordance with the optimization principle discussed in section 2.4. The tangent to the trade-off curve at $(p^*, f(p^*))$ is also shown.

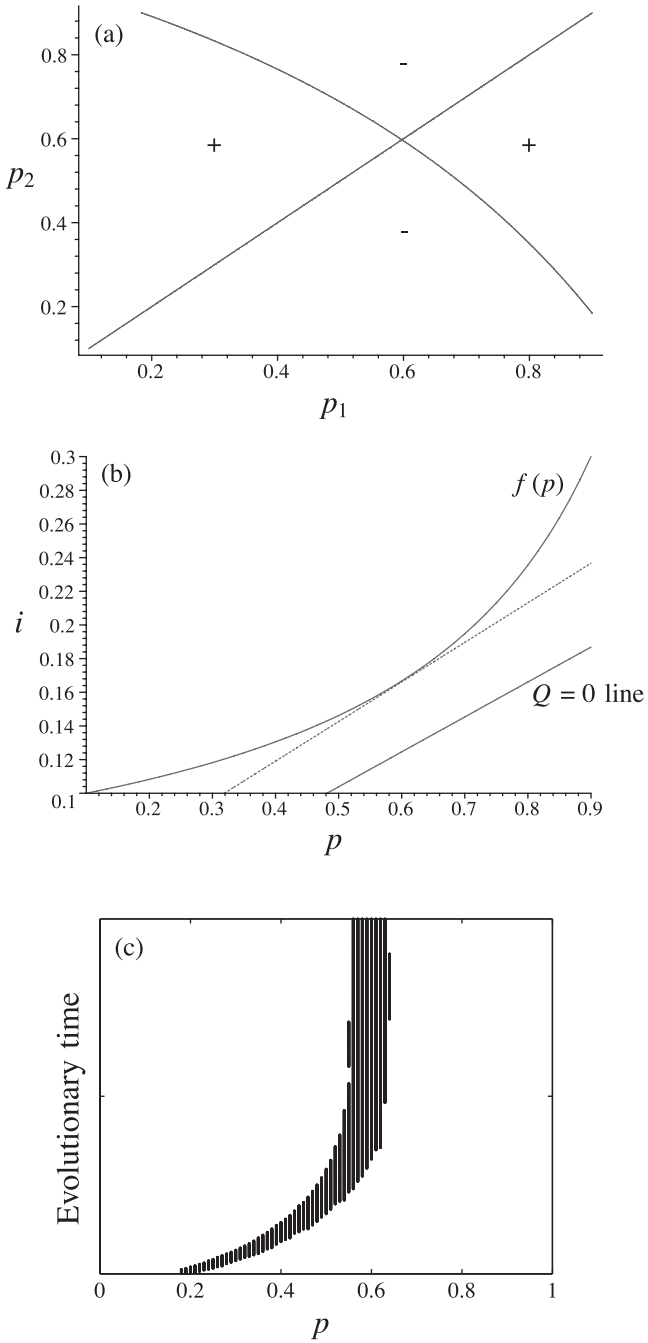

Fig. 3. An attractor singularity. (a) PIP showing the attractor at $p = 0.6$. (b) Plot of trade-off curve and the $Q = 0$ line. The tangent to the trade-off curve at the singularity is also shown. (c) Dynamical simulation. Parameter values: $\alpha = -0.7$, other parameters as in Fig. 1.

The results of a dynamical simulation for this scenario are shown in Fig. 3c. Starting with an initial resident strain with a value of p around 0.2, evolution proceeds via small mutations towards the attractor p^*.

3.2. A repellor

The PIP (Fig. 4a) shows that there is a singularity near $p = 0.24$. This time, the pattern of signs around the singularity (plus signs above and below, minus signs to the left and right) indicates that it is a repellor.

Figure 4b shows the trade-off function and the $Q = 0$ line in (p, i) space. The repellor occurs at the point that maximizes the value of $|Q|$.

The dynamical simulation illustrated in Fig. 4c shows evolution directed away from the singularity p^* and towards the extreme value $p = 0.1$.

3.3. Multiple singularities (I)

The PIP in Fig. 5a shows three singularities, which we will refer to as p_1^*, p_2^*, and p_3^* (where $p_1^* < p_2^* < p_3^*$). The central singularity p_2^* (around $p = 0.73$) is a repellor, while p_1^* and p_3^* are marginally ESS attractors.

Figure 5b shows the trade-off function and the $Q = 0$ line in (p, i) space. There are two points of intersection between the two lines, and these correspond to marginally ESS attractors. In the PIP, the singularities are the points at which the two vertical invasion boundaries intersect the main diagonal.

A dynamical simulation for this scenario is shown in Fig. 5c. Starting with an initial resident strain with a value of p close to the repellor p_2^*, evolution proceeds via small mutations away from the repellor and towards the lower attractor p_1^*.

3.4. Multiple singularities (II)

The example shown in Fig. 6 is similar to the previous example except that the curvature of the trade-off function has been changed from concave to convex. As before there is a single repellor and two marginally ESS attractors. This example and the previous one illustrate the point that if the trade-off function intersects the line $Q = 0$ at two distinct points – p_a and p_b, say (with $p_a < p_b$) – then there must be a point p_c (where $p_a < p_c < p_b$) corresponding to an evolutionary repellor.

3.5. A marginally ESS attractor

In the previous examples, we have assumed that $f' > 0$. If $f' < 0$, there will be a marginally ESS attractor at the (single) point of intersection between f and the line $Q = 0$ (if such a point exists). However, no other singularities are possible: the contours $Q = x$ in (p, i) space are straight lines with a positive gradient (as shown in Appendix B), and therefore if f has a negative slope there will be no point on f whose tangent coincides with a contour of Q, and therefore no point at which $|Q|$ is either locally maximized or locally minimized. An example of this type of scenario is shown in Fig. 7.

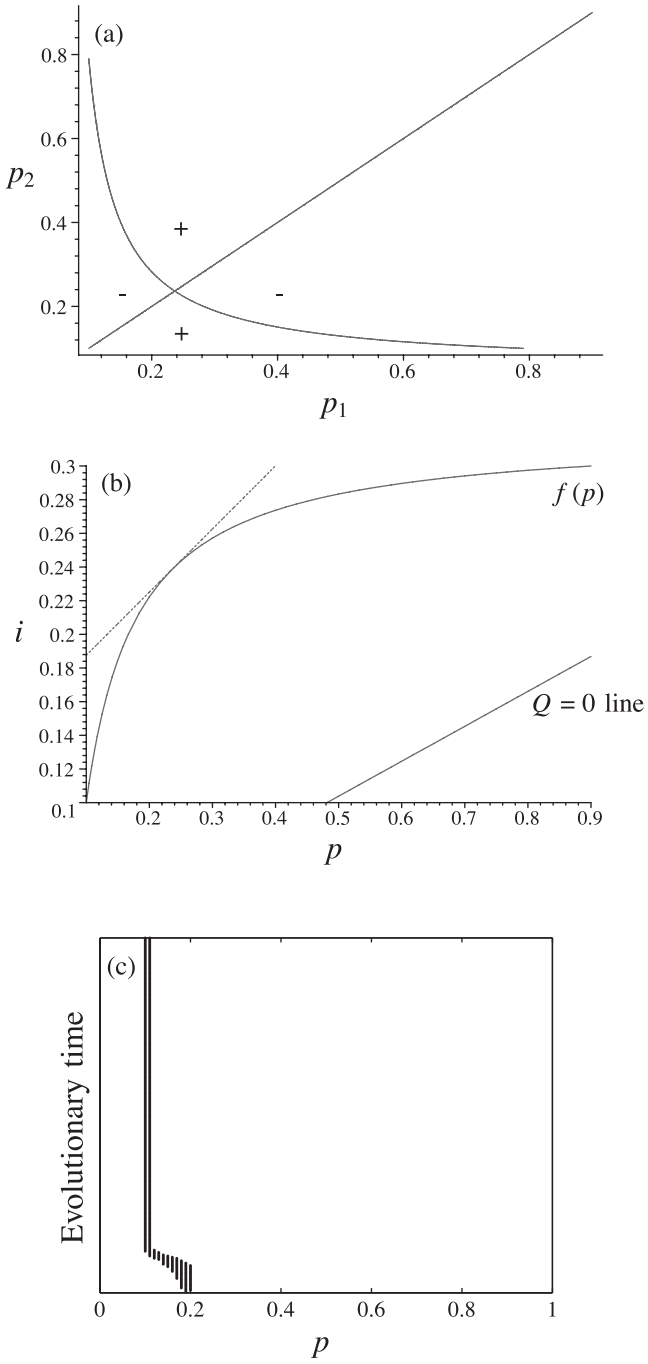

Fig. 4. A repellor singularity. (a) PIP showing the repellor at $p = 0.24$. (b) Plot of trade-off curve and the $Q = 0$ line. The tangent to the trade-off curve at the singularity is also shown. (c) Dynamical simulation. Parameter values: $\alpha = 10$, other parameters as in Fig. 1.

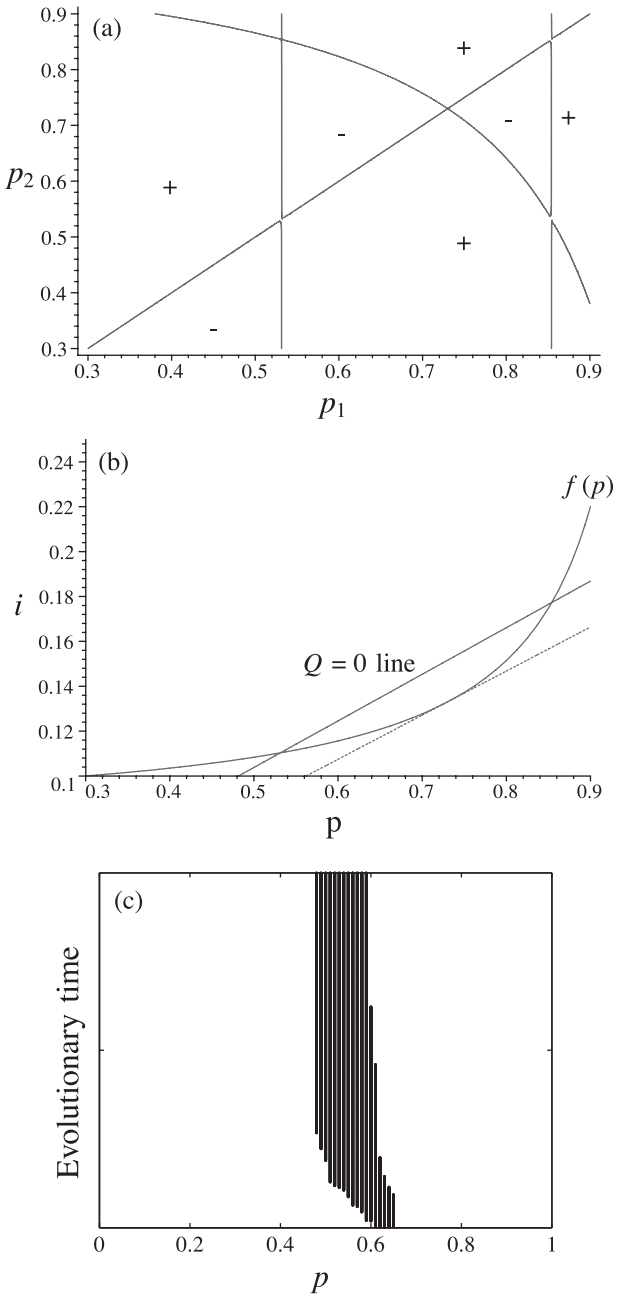

Fig. 5. Multiple singularities (I). (a) PIP showing a repellor at $p = 0.73$, and two marginally ESS attractors (at $p = 0.53$ and $p = 0.85$). (b) Plot of trade-off curve and the $Q = 0$ line. The tangent to the trade-off curve at the repellor singularity is also shown. (c) Dynamical simulation. Parameter values: $\alpha = -0.85$, other parameters as in Fig. 1.

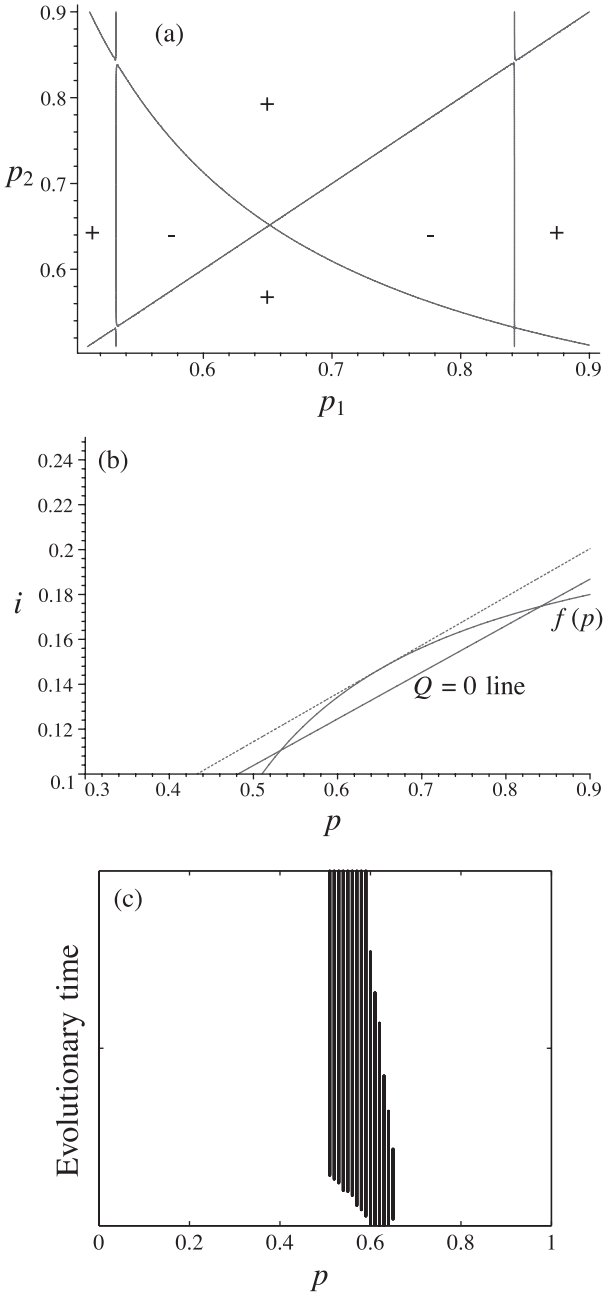

Fig. 6. Multiple singularities (II). (a) PIP showing a repellor at $p = 0.65$, and two marginally ESS attractors (at $p = 0.53$ and $p = 0.84$). (b) Plot of trade-off curve and the $Q = 0$ line. The tangent to the trade-off curve at the repellor singularity is also shown. (c) Dynamical simulation. Parameter values: $\alpha = 1.5$, other parameters as in Fig. 1.

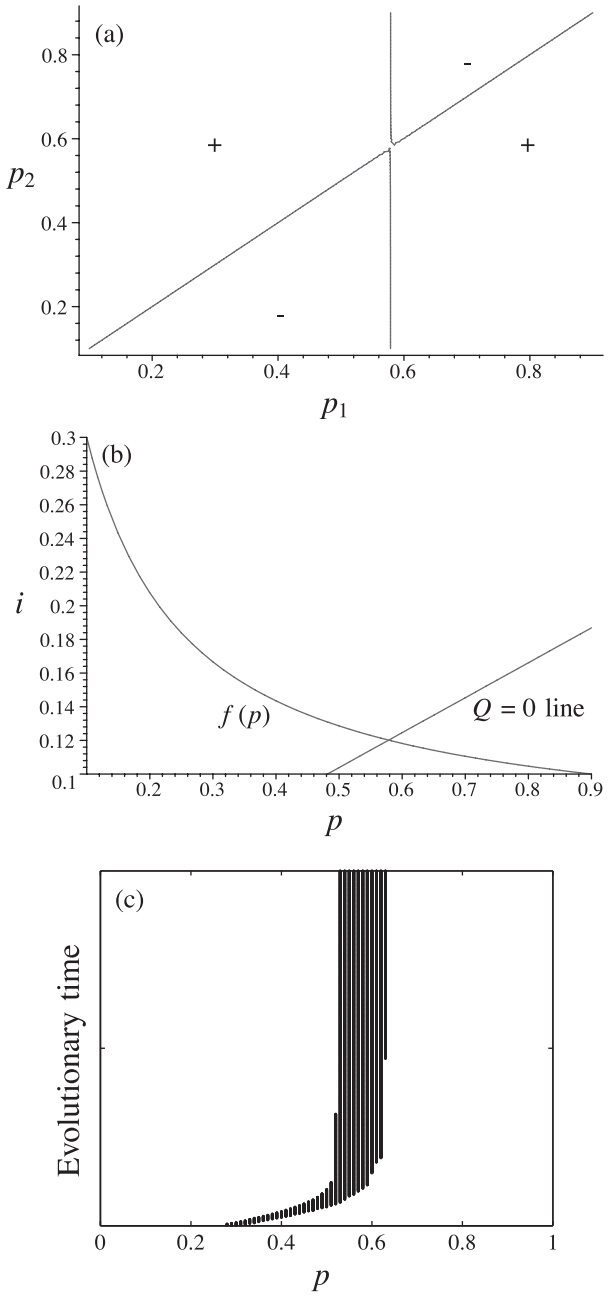

Fig. 7. Constraining i to be a decreasing function of p. (a) PIP showing a marginally ESS attractor at $p = 0.58$. (b) Plot of trade-off curve and the $Q = 0$ line. (c) Dynamical simulation. Parameter values: $\alpha = 5$, other parameters as in Fig. 1.

4. PHAGE EVOLUTION UNDER DIFFERENT ENVIRONMENTAL CONDITIONS

In this section, the function f is assumed to be a decreasing function of p, and can therefore be considered to represent a trade-off between vertical and horizontal transmission (Kaltz and Koella, 2003). Thus for a given function f there will only be one singularity, which occurs at the intersection between f and the line $Q = 0$; the singularity will be a marginally ESS attractor, as described in section 2.4.

When $Q = 0$ is satisfied, i and p cancel out of the model equations (see Appendix B). It is then possible to solve the system to give analytical expressions for R^*, S^*, L^*, and P^* in which i and p do not appear (the expressions are somewhat lengthy and are therefore not given here).

At the singularity, the ratio i^*/p^* (which is a measure of the extent to which lysis or lysogeny is favoured by the phage) is equal to the gradient of the line $Q = 0$, which is shown in Appendix B to be given by the value of the function μ, i.e. $\delta S^* P^*/L^*$ (and therefore does not depend on the actual values of i^* and p^*).

To investigate the impact of changes in the environment, we consider the input levels of susceptible bacteria (S_0) and resources (R_0) separately. Figure 8 shows what happens as S_0 increases (with R_0 fixed). In Fig. 8a, the gradient of the line $Q = 0$ increases. Thus, the intersection between f and $Q = 0$ moves in the direction of lower p and higher i. In other words, at a higher value of S_0 the singularity has a higher level of lysis and induction. In Fig. 8c, the ratio i^*/p^* is plotted against S_0. Note that the shape of the trade-off function does not affect this ratio, since the value of i^*/p^* is constant along the $Q = 0$ line as explained above.

Similarly, Fig. 9 shows that as R_0 increases (with S_0 fixed) the gradient of the line $Q = 0$ decreases, and so there is a shift towards lysogeny. Thus, the results show that an increase in the ratio of input resources to susceptible bacteria results in a shift towards lysogenic reproduction, which allows the phage population to benefit from the higher host population growth rate. On the other hand, if resources become more scarce, the phage population will achieve a fitness gain by becoming more virulent.

5. DISCUSSION

We have applied the methods of adaptive dynamics to the chemostat model of Mittler (1996). This approach has enabled us to develop and extend Mittler's work, and in particular to model the continuous evolution of temperate phage strains via small mutations.

We have shown that the location and nature of the evolutionary singularities depend on the shape of the function f (which relates the parameters i and p) and also on the position of f relative to the straight line $Q = 0$. Marginally ESS attractors occur at points of intersection between f and the $Q = 0$ line. Singularities also occur at points along f at which the value of $|Q|$ is locally maximized or locally minimized.

We have established that, in contrast to other studies in adaptive dynamics (e.g. Boots and Haraguchi, 1999; Miller *et al.*, 2005; White and Bowers, 2005), evolutionary branching does not occur in the present setting. Note that since marginally ESS attractors are located on the bifurcation point between an ESS and a branching point, a small change to the model could unfold this degeneracy into evolutionary branching. It would be instructive to carry out experimental work into the occurrence of branching in real populations of temperate phages.

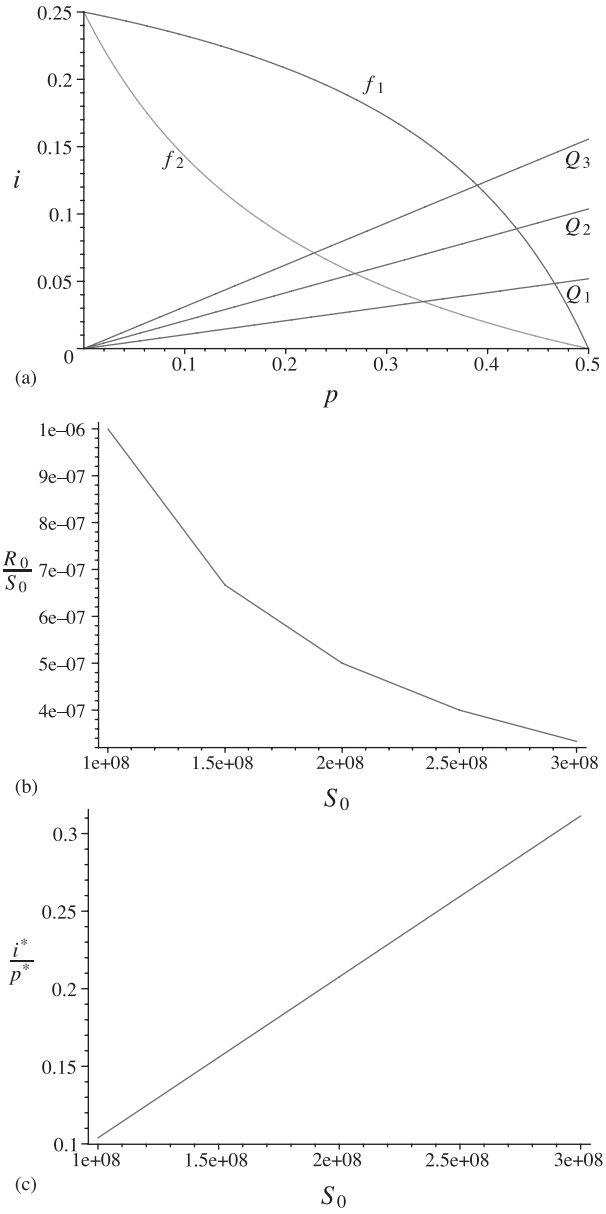

Fig. 8. Varying the input level of susceptible bacteria, S_0. As S_0 increases, the gradient of the $Q = 0$ line increases (a), so that the points at which the example trade-off functions f_1 and f_2 intersect this line change. The result is a shift towards lytic growth, as illustrated in (c); note that this figure is the same irrespective of the shape of the trade-off curve.

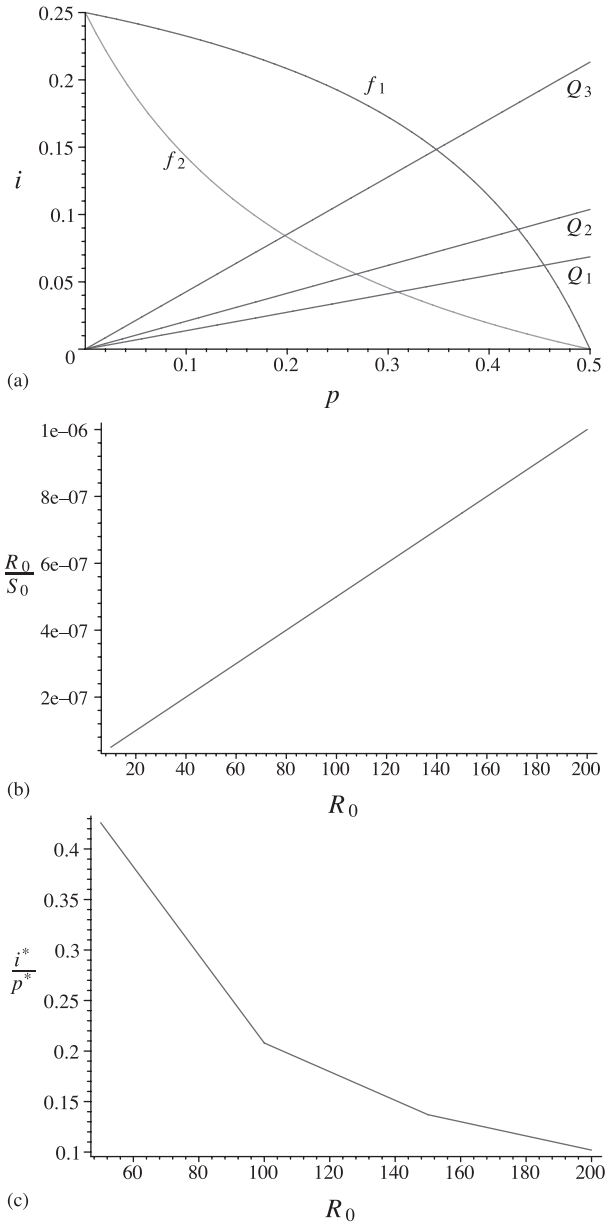

Fig. 9. Varying the input level of resources, R_0. As R_0 increases, the gradient of the $Q = 0$ line decreases (a). The result is a shift towards lysogenic growth, as illustrated in (c); as before, the shape of the trade-off curve does not affect this figure.

The gradient of the $Q = 0$ line is equal to the value of the function μ and is therefore always positive (as shown in Appendix B). However, any change in the non-evolving parameter values (e.g. the input concentrations of resources or sensitive bacteria) that alters the equilibrium levels of the populations will also alter the $Q = 0$ gradient, and possibly the nature of any singularities. For example, a repellor at which the value of Q is initially positive will become an attractor if there is a change in the parameter values that causes the slope of $Q = 0$ to decrease sufficiently (i.e. the singularity now appears on the other side of the $Q = 0$ line, so that its Q value is negative). Therefore, the choice of parameter values is particularly important in cases where singularities occur close to the $Q = 0$ line.

Provided that i is an increasing function of p, it is possible for f to intersect the line $Q = 0$ at two separate points, and these will correspond to marginally ESS attractors. When this happens, there will always be a repellor in between the two attractors, as in Figs. 6 and 7.

As mentioned in the Introduction, phage lambda and other well-studied temperate phages have evolved to have values of i and p at the lower end of the ranges of possible values. In the adaptive dynamics framework, this could occur as a result of evolution away from a repellor (as in Fig. 5). Phages with low values of i and p are likely to perform better than other phages when the environment is subject to variation, since they will be able to survive lean periods (via lysogenic infections) but also to compete strongly (via lysis) when resources and sensitive bacteria are plentiful (for a discussion of this point, see Mittler, 1996).

Whereas temperate phages are able to replicate via both the lysogenic and lytic pathways, virulent phages may only replicate via lysis. We have shown (Appendix A) that a temperate resident phage can be invaded by a virulent mutant (depending on the sign of Q_1), but a virulent resident cannot be invaded by a temperate mutant, in the present setting. This raises the question of why temperate phages emerged in the first place (assuming that they have evolved from virulent phages). The role of environmental fluctuation is likely to form part of the answer to this. Population models that include an environmental fluctuation term have been discussed by Stewart and Levin (1984) and Mittler (1996). In the present paper, we have considered a constant input of resources and sensitive bacteria to the chemostat, but it would be interesting to study models of phage evolution in the context of a fluctuating environment.

For fixed environments, it is clear that the health of the host bacterial population is an important factor in determining the optimal balance between lysis and lysogeny. If R_0 decreases, the ESS virulence increases according to Fig. 9, so scarce resources do not favour lysogeny. We have illustrated that if the phage population faces a trade-off between vertical and horizontal transmission (so that f is a decreasing function of p), changes in the relative input level of resources and susceptible bacteria result in a change in the location of the evolutionary singularity. As expected, an increase in the level of input resources per susceptible bacteria leads to a shift towards vertical transmission (via lysogeny), since the prophages receive a fitness gain from the increased growth rate of the host lysogen cell.

ACKNOWLEDGEMENTS

The authors thank Eva Kisdi for very helpful comments on a previous draft of the manuscript, which greatly improved the paper. This research was supported by the DEFRA/HEFCE Veterinary Training and Research Programme UK.

REFERENCES

Boots, M. and Haraguchi, Y. 1999. The evolution of costly resistance in host–parasite systems. *Am. Nat.*, **153**: 359–370.

Bowers, R.G. and White, A. 2002. The adaptive dynamics of Lotka-Volterra systems with trade-offs. *Math. Biosci.*, **175**: 67–81.

Bowers, R.G., Hoyle, A., White, A. and Boots, M. 2005. The geometric theory of adaptive evolution. *J. Theor. Biol.*, **233**: 363–377.

de Mazancourt, C. and Dieckmann, U. 2004. Trade-off geometries and frequency-dependent selection. *Am. Nat.*, **164**: 765–778.

Evans, T.W., Bowers R.G. and Mortimer, A.M. 2007. Modelling the stability of Stx lysogens. *J. Theor. Biol.*, **248**: 241–250.

Geritz, S.A.H., Kisdi, E., Meszena, G. and Metz, J.A.J. 1998. Evolutionarily singular strategies and the adaptive growth and branching of the evolutionary tree. *Evol. Ecol.*, **12**: 35–57.

Howe, M.M. and Bade, E.G. 1975. Molecular biology of bacteriophage Mu. *Science*, **190**: 624–632.

Kaltz, O. and Koella, J.C. 2003. Host growth conditions regulate the plasticity of horizontal and vertical transmission in *Holospora undulata*, a bacterial parasite of the protozoan *Paramecium caudatum*. *Evolution*, **57**: 1535–1542.

Kourilsky, P. 1973. Lysogenization by bacteriophage lambda. I. Multiple infection and the lysogenic response. *Molec. Gen. Genet*., **122**: 183–195.

Metz, J.A.J., Mylius, S.D. and Diekmann, O. 2008. When does evolution optimize? *Evol. Ecol.*, **10**: 629–654.

Miller, M.R., White, A. and Boots, M. 2005. The evolution of host resistance: tolerance and control as distinct strategies. *J. Theor. Biol.*, **236**: 198–207.

Mittler, J.E. 1996. Evolution of the genetic switch in temperate bacteriophage. I. Basic theory. *J. Theor. Biol.*, **179**: 161–172.

Monod, J. 1949. The growth of bacterial culture. *Annu. Rev. Microbiol.*, **3**: 371–394.

Ptashne, M. 2004. *A Genetic Switch: Phage Lambda Revisited*, 3rd edn. Cold Spring Harbor, NY: Cold Spring Harbor Laboratory Press.

Rosner, J.L. 1972. Formation, induction, and curing of bacteriophage P1 lysogens. *Virology*, **48**: 679–689.

Rueffler, C., van Dooren, T.J. and Metz, J.A.J. 2004. Adaptive walks on changing landscapes: Levins' approach extended. *Annu. Rev. Microbiol.*, **65**: 165–178.

Stewart, F.M. and Levin, B.R. 1984. The population biology of bacterial viruses: why be temperate? *Theor. Pop. Biol.*, **26**: 93–117.

White, A. and Bowers, R.G. 2005. Adaptive dynamics of Lotka-Volterra systems with trade-offs: the role of interspecific parameter dependence in branching. *Math. Biosci.*, **193**: 101–117.

White, A., Greenman, J.V., Benton, T.G. and Boots, M. 2006. Evolutionary behaviour in ecological systems with trade-offs and non-equilibrium population dynamics. *Evol. Ecol. Res.*, **8**: 387–398.

APPENDIX A: THE FITNESS FUNCTION

Here we present an outline of the method used to derive the fitness function $s_{p1}(p_2)$. The method follows Mittler (1996), but is applied to the amended version of the model, which includes an allowance for the loss of phage particles that adsorb to and infect susceptible cells, as discussed in the main text.

Let R^*, S^*, L_1^*, and P_1^* be the equilibrium values of R, S, L_1, and P_1 calculated from equations (1), (2), (3), and (5) respectively, with $L_2 = P_2 = 0$. To see what will happen if a small number of mutant type 2 phages and lysogens emerge, we can consider the linearized system

$$\frac{dL_2}{dt} = [rR^*/(R^* + k) - i_2 - \xi - \omega]L_2 + [p_2\delta S^*]P_2$$

$$\frac{dP_2}{dt} = [\beta i_2]L_2 + [\beta(1 - p_2)\delta S^* - \delta(S^* + L_1^*) - \omega]P_2$$

Now we assume that p_2 and i_2 are both greater than zero. Strain 2 and its lysogen can invade when rare if the above system has at least one positive eigenvalue. The eigenvalues are the solutions of

$$(a - \lambda)(d - \lambda) - bc = 0,$$

where $a = rR^*/(R^* + k) - i_2 - \xi - \omega$, $b = p_2\delta S^*$, $c = \beta i_2$, and $d = \beta(1 - p_2)\delta S^* - \delta(S^* + L_1^*) - \omega$. There will be a positive eigenvalue if $ad < bc$ or $(a + d) > 0$, or both. In fact, it will be shown below that it is only necessary to consider the condition $ad < bc$.

Let $A = a + i_2 = rR^*/(R^* + k) - \xi - \omega$ and $D = d + p_2\beta\delta S^* = \beta\delta S^* - \delta(S^* + L_1^*) - \omega$. Setting equations (3) and (5) equal to zero (with $P_2 = L_2 = 0$), we obtain $A = -(P_1^*/\beta L_1^*)D$. So A and D have opposite signs, and given that $a = A - i_2$ and $d = D - p_2\beta\delta S^*$, it is not possible for both a and d to be positive.

If one of a and d is positive and the other is negative, we must have $ad < bc$ (since b and c are always positive), and therefore there will certainly be a positive eigenvalue. If both a and d are negative, $a + d < 0$, and so there will only be a positive eigenvalue if $ad < bc$ holds. Thus, checking the condition $ad < bc$ covers all possibilities.

Given the above definitions of A and D, the condition $ad < bc$ implies

$$p_2\delta S^*\beta i_2 - (A - i_2)(D - p_2\beta\delta S^*) > 0$$

Using the relationship $A = -(P_1^*/\beta L_1^*)D$ (from above) and re-arranging, we obtain:

$$A^2\beta L_1^*/P_1^* - (\beta L_1^* A/P_1^*)i_2 + \beta\delta S^* A p_2 > 0$$

Now define Q_1, μ_1, and γ_1 as follows: $Q_1 = -\beta L_1 A/P_1^*$; $\mu_1 = \delta S^* P_1^*/L_1^*$; $\gamma_1 = P_1^*/\beta L_1^*$. Then the above condition can be written as:

$$Q_1^2\gamma_1 + Q_1 i_2 - Q_1\mu_1 p_2 > 0$$

The left-hand side of the above expression is the fitness function given in equation (7) in the text. The expression $Q_1 = (\beta p\delta P_1^* S^* - \beta i L_1^*)/P_1$ is obtained by setting equation (3) equal to zero and solving for A.

In the special case of a virulent mutant, i.e. $p_2 = 0$, there are no L_2 lysogens and there is a single invasion eigenvalue, $\lambda = \beta\delta S^* - \delta(S^* + L_1^*) - \omega = Q_1$. Therefore, a resident strain can be invaded by a virulent mutant if $Q_1 > 0$; on the other hand, if $Q_1 < 0$, a virulent mutant cannot invade.

In the special case where the resident phage is virulent, i.e. $p_1 = 0$, then $Q_1 = 0$ and so the fitness of an invading mutant (i.e. $Q_1^2\gamma_1 + Q_1 i_2 - Q_1\mu_1 p_2$) will be zero for any values of p_2 and i_2. Therefore, no mutant phage can invade.

APPENDIX B: THE Q FUNCTION

Here we show that given a real number x, the line $Q(p, i) = x$ (if it exists) is linear in (p, i) space. Setting the right-hand sides of equations (1), (2), (3), and (5) all equal to zero (with $P_2 = L_2 = 0$), and using the relationship $Q(p, i) = x$, we obtain:

$$0 = \omega(R_0 - R^*) - \varepsilon r(S^* + L_1^*)R^*/(R^* + k)$$

$$0 = \omega(S_0 - S^*) - rS^*R^*/(R^* + k) + \xi L_1^* - \delta S^* P_1^*$$

$$0 = x + \frac{\beta r L_1 R}{P_1(R + k)} - \frac{\beta \xi L_1}{P_1} - \frac{\beta \omega L_1}{P_1}$$

$$0 = -x + \beta\delta S - \delta L_1 - \omega$$

Since p and i do not appear in the above equations, the values of R^*, S^*, L_1^*, and P_1^* are constant along the line $Q(p, i) = x$.

Since $Q(p, i) = (\beta p_1 \delta P_1^* S^* - \beta i_1 L_1^*)/P_1^*$, the line $Q(p, i) = x$ must be a straight line with gradient $\delta P_1^* S^*/L_1^*$ and intercept $-xP_1/(\beta L_1)$ (where R^*, S^*, L_1^*, and P_1^* are obtained from the four equations above). Note that the gradient is equal to the value of the function μ, and that all points along the line $Q(p, i) = x$ must have the same value of μ.

To show that $Q(p, i)$ is positive for all points below the line $Q(p, i) = 0$, we can consider the single point $(p, 0)$, where $0 < p < 1$. At this point, we have $Q = (\beta p \delta S^* P_1^*)/P_1^* > 0$.

To show that $Q(p, i)$ is negative for all points above the line $Q(p, i) = 0$, we can consider the single point $(0, i)$, where $i > 0$. At this point, we have $Q = -\beta i_1 L_1^*/P_1^* < 0$.